frontiers in Physics

ORIGINAL RESEARCH
published: 16 February 2022
doi: 10.3389/fphy.2022.847649

Propagation Properties of a Twisted Hermite-Gaussian Correlated Schell-Model Beam in Free Space

Leixin Liu[1], Haiyun Wang[1], Lin Liu[1], Yiming Dong[2], Fei Wang[1], Bernhard J. Hoenders[3], Yahong Chen[1], Yangjian Cai[1,4,5] and Xiaofeng Peng[4,5]**

[1]School of Physical Science and Technology, Soochow University, Suzhou, China, [2]Department of Physics, Shaoxing University, Shaoxing, China, [3]Zernike Institute for Advanced Materials, University of Groningen, Groningen, Netherlands, [4]School of Physics and Electronics, Shandong Normal University, Jinan, China, [5]Shandong Provincial Engineering and Technical Center of Light Manipulation and Shandong Provincial, Key Laboratory of Optics and Photonic Devices, School of Physics and Electronics, Shandong Normal University, Jinan, China

We introduce a novel type of twisted partially coherent beams with a nonconventional correlation function, named the twisted Hermite-Gaussian correlated Schell-model (THGCSM) beam. The condition that a twist phase can be imposed on a partially coherent beam is addressed for Schell-model fields endowed with rectangular symmetry. Further, the analytical formula for the THGCSM beam propagating in free space has been derived with the help of the generalized Collins formula. The propagation properties, such as the spectral density and the spectral degree of coherence (SDOC) of the THGCSM beam, also have been studied in detail by some numerical examples. The numerical results show that the twist phase plays a role in resisting beam splitting, caused by the correlation structure, and induces the rotation of the distribution of the SDOC on propagation. Moreover, it is interesting to find that when the beam carries a twist phase, this will endow the beam the ability to maintain its distribution of the SDOC on propagation and enhance the self -reconstruction capability of the SDOC. Our results may provide new insights into nonconventional partially coherent beams with twisted phase and may be useful in some applications, such as optical communications and information recovery.

Keywords: self-reconstruction, spectral degree of coherence, twist phase, propagation properties, partially coherent

OPEN ACCESS

Edited by:
Shangran Xie,
Beijing Institute of Technology, China

Reviewed by:
Xinglin Zeng,
Max Planck Institute for the Science of Light, Germany
Yang Chen,
Paul Scherrer Institut (PSI), Switzerland

****Correspondence:***
Yangjian Cai
yangjiancai@suda.edu.cn
Xiaofeng Peng
xfpeng888@163.com

Specialty section:
This article was submitted to Optics and Photonics, a section of the journal Frontiers in Physics

Received: *03 January 2022*
Accepted: *18 January 2022*
Published: *16 February 2022*

Citation:
Liu L, Wang H, Liu L, Dong Y, Wang F, Hoenders BJ, Chen Y, Cai Y and Peng X (2022) Propagation Properties of a Twisted Hermite-Gaussian Correlated Schell-Model Beam in Free Space. Front. Phys. 10:847649. doi: 10.3389/fphy.2022.847649

INTRODUCTION

Coherence is one of the most notable features of a laser beam. These light beams (i.e., partially coherent beam) have attracted intensive attentions due to their wide applications in inertial confinement fusion, ghost imaging, sub-Rayleigh imaging, particle trapping, free space optical communications and optical scattering [1–8]. Furthermore, Gori et al. [9, 10] proposed the sufficient conditions for designing a real genuine cross-spectral density function or matrix of a partially coherent beam. Based on the above works, a variety of partially coherent beams with nonconventional correlation functions (i.e., the correlation function doesn't satisfy the Gaussian distribution) have been introduced theoretically and generated experimentally [11–27]. It is found that beams with nonconventional correlation functions will exhibit unique properties on propagation, such as self-splitting, self-reconstruction, locally sharpened and laterally shifted

intensity maxima [13, 22, 27], which are useful in multi-particles trapping, atoms guiding, image transfer and recovery. Moreover, the beam profiles in the focal plane (or far fields) can be controlled by endowing the beam with a specific correlation function [15–19, 26], for example, dark-hollow beam profiles (or an optical cage) can be formed near the focal plane when the correlation function satisfies a Laguerre–Gaussian distribution [18]. A Multi-Gaussian correlated Schell-model beam would generate a rectangular intensity profile in the focal plane, and a ring-shaped beam and controllable intensity lattices also can be achieved with the help of the correlation functions [15, 26]. In addition, partially coherent beams with prescribed correlation functions can be applied to reduce scintillation in turbulence [28], overcome the classical Rayleigh diffraction limit [29], coherence-based optical encryption [30], robust microscopy imaging [31], robust far-field imaging [32], and optical beam shaping [33].

On the other hand, partially coherent beams with a twist phase (i.e., twisted partially coherent beam) carry orbital angular momentum (OAM) [34]. Twist phase as a "genuinely two-dimensional" phase can't exist in a coherent beam and its value is bounded in strength. Twist phase was introduced by Simon et al. in 1993 and has been demonstrated in an experiment by Friberg [35, 36]. Due to the intrinsic chiral property of the twist phase the rotation of the beam spot on propagation is induced, and both the distribution of the SDOC, the degree of polarization and the state of polarization of the beam on propagation are affected [37, 38]. Besides, light beams with a twist phase have advantages in resisting coherence (or turbulence)-induced degeneration, depolarization and overcoming the classical Rayleigh limit [37, 39]. It is shown in [40, 41] that using a twist phase can greatly increase the amount of OAM of a partially coherent vortex beam and enhance its self-reconstruction capability.

Recently, some new ways have been introduced to generate twisted Gaussian Schell-model beams and measure their orbital angular momentum [42, 43]. The problem of when a twist phase can be imposed on a partially coherent beam, generated from a Schell-model source with axial symmetries, was explored in [44, 45]. Two approaches have been proposed to devise genuine twist beams with and without symmetry [46, 47]. In this paper, we devised a newly twisted partially coherent beam named the twisted Hermite-Gaussian correlated Schell-model (THGCSM) beam. The condition that the THGCSM beam will be bona fide is met, and the propagation properties of the THGCSM beam have been investigated in detail. Our results show that the twist phase plays a role of preventing deterioration of the intensity distribution and induces rotation of the distribution of the SDOC around the axis on propagation. Furthermore, the twist phase also will enhance the ability of the beam to maintain the distribution of the SDOC and its self-reconstruction capability, which will be useful for optical information processing and recovery.

THEORY OF THE TWISTED HERMITE-GAUSSIAN CORRELATED SCHELL-MODEL BEAM

Twisted Schell-Model Beams With Rectangular Symmetry

Based on the unified theory of coherence and polarization, the statistical properties of a partially coherent beam can be characterized by the cross-spectral density (CSD) [48]. For Schell-model fields, endowed with rectangular symmetry, the cross-spectral density (CSD) of the beam can be expressed as

$$W_0\ (\boldsymbol{r_1}, \boldsymbol{r_2}) = \tau^*(\boldsymbol{r_1})\tau(\boldsymbol{r_2})\, u(|x_1 - x_2|)\, u(|y_1 - y_2|), \quad (1)$$

where $\boldsymbol{r_1} = (x_1, y_1)$, $\boldsymbol{r_2} = (x_2, y_2)$ are two arbitrary transverse position vectors, τ (r_i) denotes the transmission function of an arbitrary (complex) amplitude filter and u ($|x_1$-$x_2|$)u ($|y_1$-$y_2|$) is the spectral degree of coherence. When the beam carries a twist phase, the CSD is defined as

$$W_{0u}\ (\boldsymbol{r_1}, \boldsymbol{r_2}) = \tau^*(\boldsymbol{r_1})\tau(\boldsymbol{r_2})\, u(|x_1 - x_2|)\, u(|y_1 - y_2|)\, exp(-ik\mu_0 \boldsymbol{r_1} \times \boldsymbol{r_2}), \quad (2)$$

where the last exponential term represents the twist phase, with μ_0 being the twist factor. According to the Refs. [44, 45], the CSD will be bona fide, if and only if the corresponding uniform source, defined as

$$W_u\ (\boldsymbol{r_1}, \boldsymbol{r_2}) = u(|x_1 - x_2|)\, u(|y_1 - y_2|)\, exp(-ik\mu_0 \boldsymbol{r_1} \times \boldsymbol{r_2}), \quad (3)$$

is bona fide too. Then, we find that the uniform source satisfies the following formal integral relationship

$$\int d^2\rho W_u(\boldsymbol{r_1}, \boldsymbol{\rho}) T_u(\boldsymbol{\rho}, \boldsymbol{r_2}) = \int d^2\rho T_u(\boldsymbol{r_1}, \boldsymbol{\rho}) W_u(\boldsymbol{\rho}, \boldsymbol{r_2}), \quad (4)$$

for any pair $(\boldsymbol{r_1}, \boldsymbol{r_2})$, $\boldsymbol{\rho} = (\rho_x, \rho_y)$ is an arbitrary transverse position vector, and $T_u = exp(-ik\mu_0 \boldsymbol{r_1} \times \boldsymbol{r_2})$ denotes the twist phase. To prove this, on substituting **Eq. 3** into **Equation 4**, the l. h. s of **Eq. 4** reads as follows

$$\int d^2\rho W_u(\boldsymbol{r_1}, \boldsymbol{\rho}) T_u(\boldsymbol{\rho}, \boldsymbol{r_2}) = \int d^2\rho\, u(|x_1 - \rho_x|)\, u(|y_1 - \rho_y|)\, exp(-ik\mu_0 (\boldsymbol{r_1} - \boldsymbol{r_2}) \times \boldsymbol{\rho}), \quad (5)$$

For the r. h. s of **Eq. 4** we obtain:

$$\int d^2\rho T_u(\boldsymbol{r_1}, \boldsymbol{\rho}) W_u(\boldsymbol{\rho}, \boldsymbol{r_2}) = \int d^2\rho\, u(|\rho_x - x_2|)\, u(|\rho_y - y_2|)\, exp(-ik\mu_0 (\boldsymbol{r_1} - \boldsymbol{r_2}) \times \boldsymbol{\rho}), \quad (6)$$

Then, taking into account that $\exp[-ik\mu_0 (\boldsymbol{r_1} - \boldsymbol{r_2}) \times \boldsymbol{\rho}] = \exp[-ik\mu_0 (\boldsymbol{r_1} - \boldsymbol{r_2}) \times (\boldsymbol{\rho} - (\boldsymbol{r_2} - \boldsymbol{r_1}))]$,

Eq. 6 can be expressed as follows

$$\int d^2\rho T_u(\boldsymbol{r_1}, \boldsymbol{\rho}) W_u(\boldsymbol{\rho}, \boldsymbol{r_2}) = \int d^2\rho\, u(|\rho_x - (x_2 - x_1) - x_1|)\, u(|\rho_y - (y_2 - y_1) - y_1|) \times exp[-ik\mu_0 (\boldsymbol{r_1} - \boldsymbol{r_2}) \times (\boldsymbol{\rho} - (\boldsymbol{r_2} - \boldsymbol{r_1}))]. \quad (7)$$

On letting $\boldsymbol{\rho} = \boldsymbol{\rho} - (\boldsymbol{r}_2 - \boldsymbol{r}_1)$, **Eq. 7** can be recast as

$$\int d^2\rho T_u(\boldsymbol{r}_1, \boldsymbol{\rho}) W_u(\boldsymbol{\rho}, \boldsymbol{r}_2) = \int d^2\rho\, u\left(\left|\rho_x - x_1\right|\right) u\left(\left|\rho_y - y_1\right|\right) exp[-ik\mu_0(\boldsymbol{r}_1 - \boldsymbol{r}_2) \times \boldsymbol{\rho}]. \quad (8)$$

Thus, the **Equation 4** has been proved. Moreover, it has been mentioned in [45], when the **Equation 4** is satisfied, the uniform source W_u defined by **Eq. 3** and the twist phase T_u share the same coherent modes, defined as

$$\Phi_{j,m}(r) = \sqrt{\frac{u}{\pi}}\left[\frac{(j-|m|)!}{(j+|m|)!}\right]^{1/2} (r\sqrt{u})^{2|m|} exp(i2m\varphi) L_{j-|m|}^{2|m|}(ur^2) exp\left(-\frac{ur^2}{2}\right), \quad (9)$$

with $u = k\mu_0$, $k = 2\pi/\lambda$ is the wavenumber with wavelength λ, and $j = 0, 1/2, 1, \ldots, m = -j, j+1, \ldots, j$. Here, $L_{j-|m|}^{2|m|}$ is the Laguerre polynomials with the radial index j-$|m|$ and the angular index $2|m|$, while exp $(i2m\varphi)$ represents the vortex phase.

If the uniform source W_u is bona fide, the sufficient condition is that the eigenvalue sequence $\{\lambda_{j,m}\}$ should be nonnegative. These eigenvalues are defined as

$$\lambda_{j,m} = \iint d^2\boldsymbol{r}_1 \boldsymbol{r}_2 W_u(\boldsymbol{r}_1, \boldsymbol{r}_2) \Phi_{j,m}(\boldsymbol{r}_1) \Phi_{j,m}^*(\boldsymbol{r}_2). \quad (10)$$

On substituting **equations 3** and **(9)** into **Equation 10**, and on letting $\boldsymbol{r}_1 - \boldsymbol{r}_2 = \boldsymbol{r}$, we have

$$\lambda_{j,m} = \int d^2 r u(x) u(y) \int d^2 r_2 exp(-ik\mu_0 \boldsymbol{r} \times \boldsymbol{r}_2) \Phi_{j,m}(\boldsymbol{r} + \boldsymbol{r}_2) \Phi_{j,m}^*(\boldsymbol{r}_2). \quad (11)$$

Use the Following Expression [45]

$$\int d^2 r_2\, exp(-ik\mu_0 \boldsymbol{r} \times \boldsymbol{r}_2) \Phi_{j,m}(\boldsymbol{r} + \boldsymbol{r}_2) \Phi_{j,m}^*(\boldsymbol{r}_2) = \mathcal{L}_{j+m}(ur^2), \quad (12)$$

with $\mathcal{L}_n(x) = L_n(x) exp(-x/2)$, and $\lambda_{j,m} = \lambda_{j+m} = \Lambda_b$. After some operation, we have

$$\Lambda_b = \sum_{k0=0}^{b} \int u(x) L_{k0}^{-1/2}(ux^2) exp\left(-\frac{ux^2}{2}\right) dx \times \int u(y) L_{b-k0}^{-1/2}(uy^2) exp\left(-\frac{uy^2}{2}\right) dy. \quad (13)$$

Eq. 13 is one of the main results of this paper, which can be used to assess the conditions when the Schell-model beams with rectangular symmetry can carry the twist phase.

Analytical Formula for a Twisted Hermite-Gaussian Correlated Schell-Model Beam

In this section, we introduce a new kind of twisted partially coherent beam with nonconventional correlation function, named the twisted Hermite-Gaussian correlated Schell-model (THGCSM) beam. As a natural extension of the Hermite-Gaussian correlated Schell-model (HGCSM) beam [22], the CSD in the source plane ($z = 0$) is defined as

$$W(\boldsymbol{r}_1, \boldsymbol{r}_2) = \exp\left(\frac{\boldsymbol{r}_1^2 + \boldsymbol{r}_2^2}{4\sigma_0^2}\right) \frac{H_{2m}[(x_2 - x_1)/\sqrt{2}\delta_0]}{H_{2m}[0]} \exp\left[-\frac{(x_2 - x_1)^2}{2\delta_0^2}\right] \times \frac{H_{2n}\left[\frac{(y_2 - y_1)}{\sqrt{2}\,\delta_0}\right]}{H_{2n}[0]} \exp\left[-\frac{(y_2 - y_1)^2}{2\delta_0^2}\right] \exp(-ik\mu_0 \boldsymbol{r}_1 \times \boldsymbol{r}_2), \quad (14)$$

where $\boldsymbol{r}_1 = (x_1, y_1)$, $\boldsymbol{r}_2 = (x_2, y_2)$ are two arbitrary transverse position vectors in the source plane, σ_0 and δ_0 represent the beam width and the spatial coherence width, respectively. H_{2m} and H_{2n} are the Hermite polynomial of order 2m and 2n, respectively. After some algebra, **Equation 14** can be expressed in the following alternative form

$$W(\boldsymbol{r}_1, \boldsymbol{r}_2) = \frac{m!\sqrt{\pi}}{\Gamma(m + 1/2)} \frac{n!\sqrt{\pi}}{\Gamma(n + 1/2)} exp\left(\frac{r_1^2 + r_2^2}{4\sigma_0^2}\right) L_m^{-1/2} \left[-\frac{(x_2 - x_1)^2}{2\delta_0^2}\right] exp\left[-\frac{(x_2 - x_1)^2}{2\delta_0^2}\right] \times L_n^{-1/2}\left[-\frac{(y_2 - y_1)^2}{2\delta_0^2}\right] exp\left[-\frac{(y_2 - y_1)^2}{2\delta_0^2}\right] exp(-ik\mu_0 \boldsymbol{r}_1 \times \boldsymbol{r}_2). \quad (15)$$

As mentioned in **section 2.1**, the THGCSM beam will be bona fide, if and only if the corresponding uniform source, defined as

$$W_{u0}(\boldsymbol{r}_1, \boldsymbol{r}_2) = L_m^{-1/2}\left[-\frac{(x_2 - x_1)^2}{2\delta_0^2}\right] exp\left[-\frac{(x_2 - x_1)^2}{2\delta_0^2}\right] \times L_n^{-1/2}\left[-\frac{(y_2 - y_1)^2}{2\delta_0^2}\right] exp\left[-\frac{(y_2 - y_1)^2}{2\delta_0^2}\right] exp(-ik\mu_0 \boldsymbol{r}_1 \times \boldsymbol{r}_2). \quad (16)$$

is bona fide too. On substituting **Equation 15** into **Equation 10**, and after some tedious integrations and algebraic manipulations, we have

$$\Lambda_b = \sum_{k0=0}^{b} \frac{2\delta_0^2}{1 + u\delta_0^2} \frac{\Gamma(m + k0 + 1/2)\Gamma(n + b - k0 + 1/2)}{m!k!n!(b - k0)!} \left(\frac{u\delta_0^2}{1 + u\delta_0^2}\right)^{m+n} \left(\frac{1 - u\delta_0^2}{1 + u\delta_0^2}\right)^{b} \times {}_2F_1\left[-m, -k0; -m - k0 + \frac{1}{2}; -\frac{(1 + u\delta_0^2)}{(1 - u\delta_0^2)}\right] \times {}_2F_1\left[-n, k0 - b; k0 - b - n + \frac{1}{2}, -\frac{(1 + u\delta_0^2)}{1 - u\delta_0^2}\right], \quad (17)$$

where ${}_2F_1$ is a hypergeometric function. So, in order for W_u to be bona fide (i.e., $\lambda_{j,m}$ should be nonnegative), the parameter $u = k\mu_0$ in **Eq. 17** must be bounded by the following inequality:

$$u\delta_0^2 \leq 1. \quad (18)$$

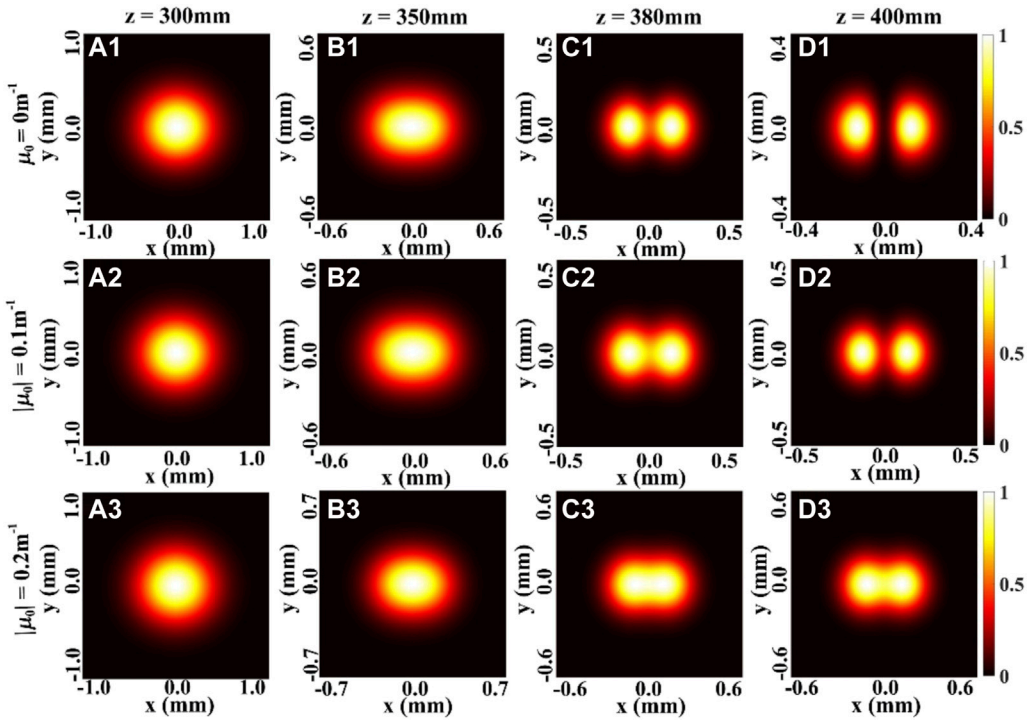

FIGURE 1 | Density plot of the normalized spectral density of a focused THGCSM beam with $m = 1$, $n = 0$ for different values of the twist factor μ_0 at several propagation distances.

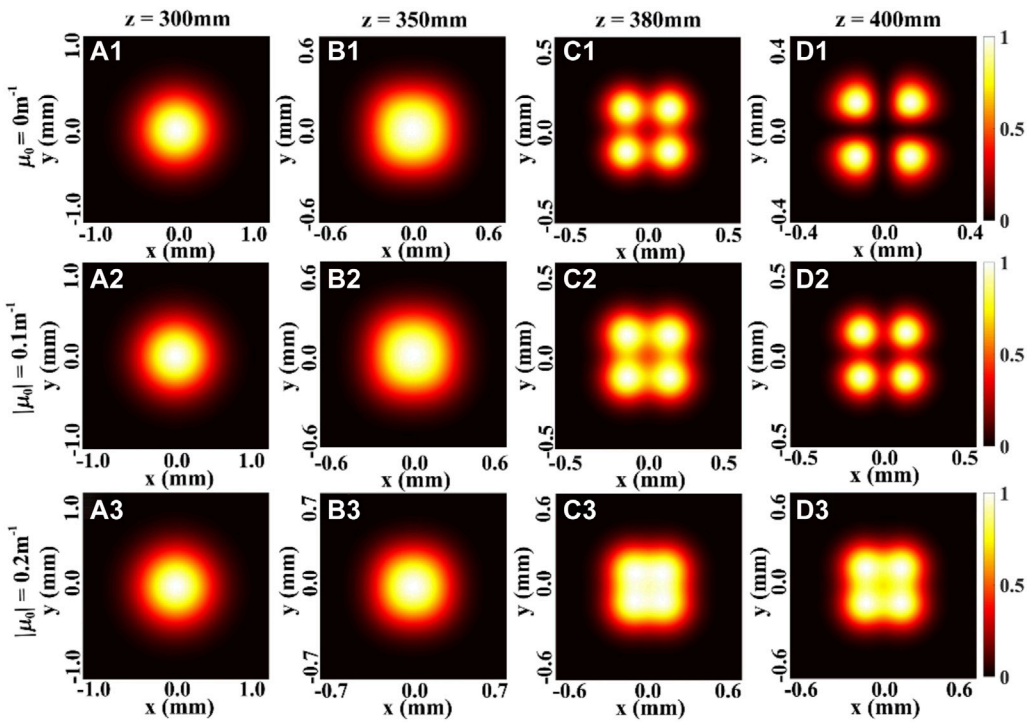

FIGURE 2 | Density plot of the normalized spectral density of a focused THGCSM beam with $m = 1$, $n = 1$ for different values of the twist factor μ_0 at several propagation distances.

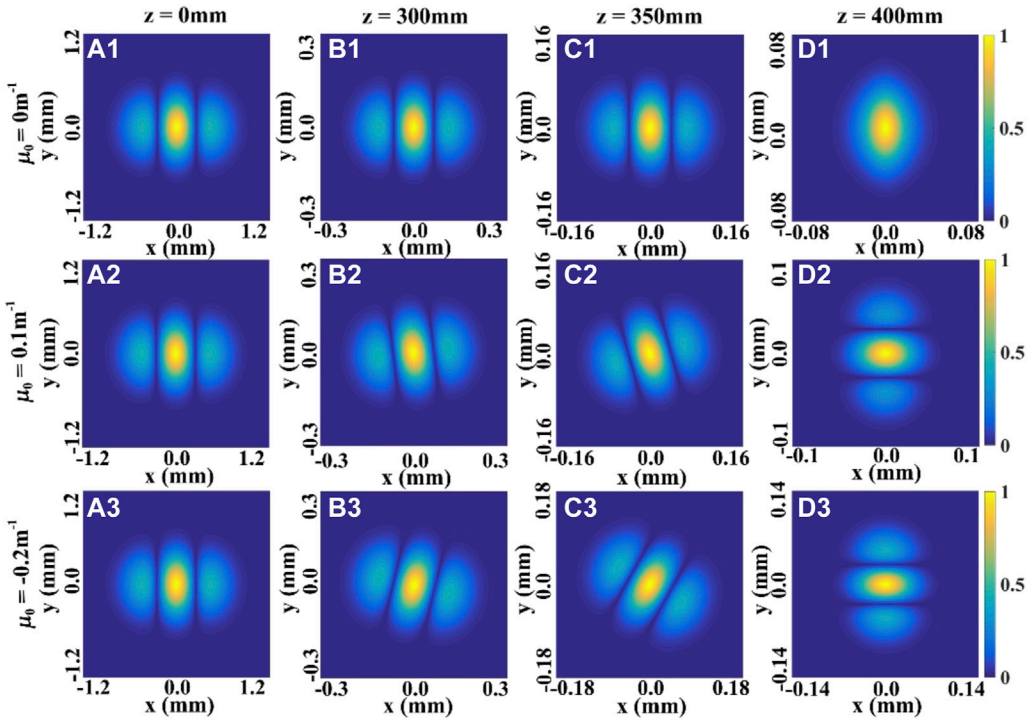

FIGURE 3 | Modulus of the SDOC between two points $\boldsymbol{\rho}$ and$-\boldsymbol{\rho}$ of the THGCSM beam with $m = 1$, $n = 0$ for different values of the twist factor μ_0 at several propagation distances.

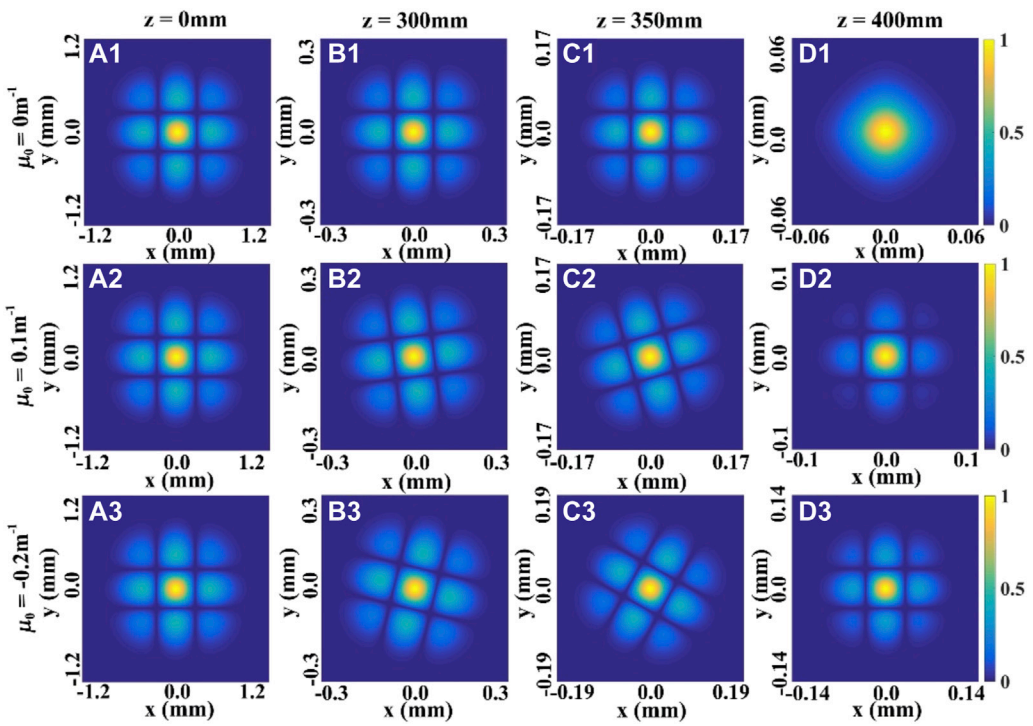

FIGURE 4 | Modulus of the SDOC between two points $\boldsymbol{\rho}$ and $-\boldsymbol{\rho}$ of the THGCSM beam with $m = 1$, $n = 1$ for different values of the twist factor μ_0 at several propagation distances.

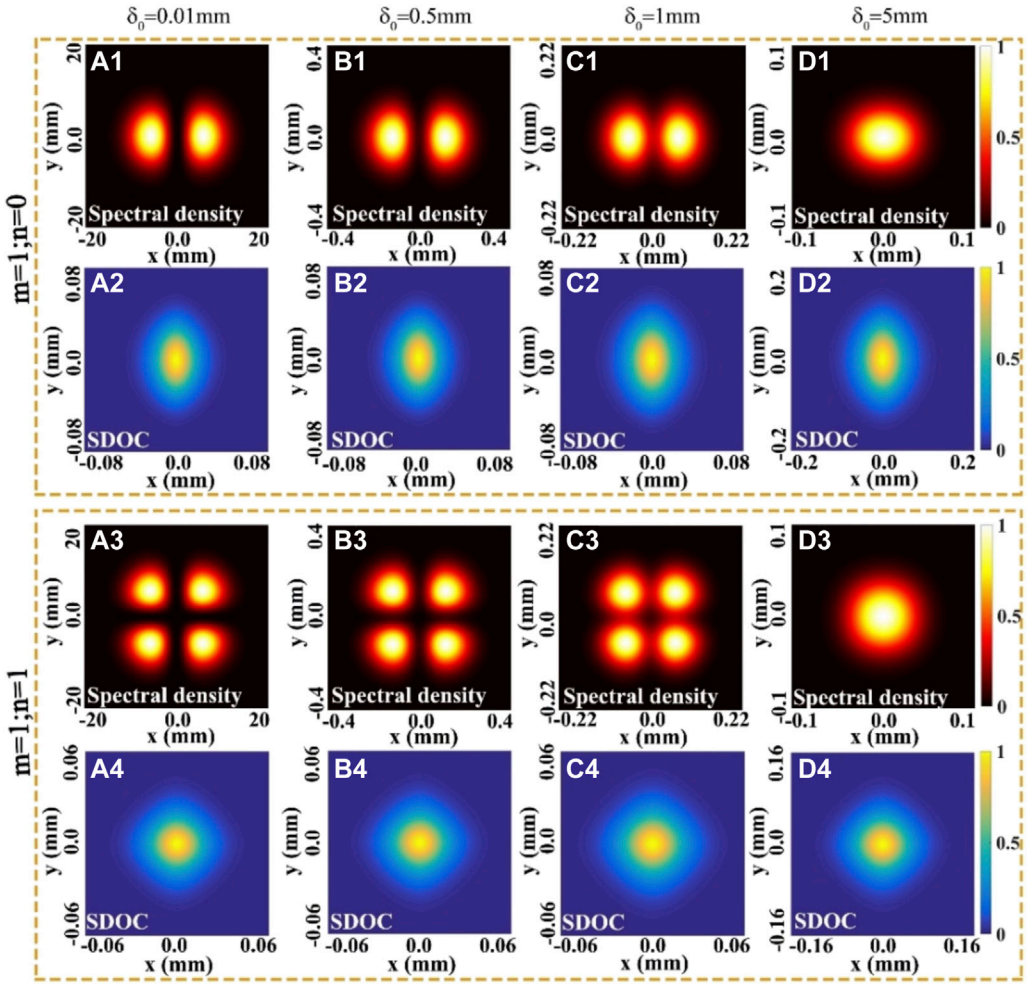

FIGURE 5 | Density plots of the normalized spectral density and the modulus of the SDOC ($|\eta(\boldsymbol{\rho},-\boldsymbol{\rho})|$) of a focused HGCSM beam for different values of the spatial coherence width δ_0 in the focal plane.

Thus, the THGCSM beam will be bona fide, if and only if the **Equation 18** is satisfied. Then, the propagation of the THGCSM beam through an ABCD optical system can be investigated with the help of the generalized Collins formula [38, 40].

$$W(\boldsymbol{\rho}_1,\boldsymbol{\rho}_2;z)=\frac{1}{(\lambda B)^2}exp\left[-\frac{ikD}{2B}\left(\rho_1^2-\rho_2^2\right)\right]\int_{-\infty}^{\infty}\int_{-\infty}^{\infty}W(\boldsymbol{r}_1,\boldsymbol{r}_2)\times exp\left[-\frac{ikA}{2B}\left(\boldsymbol{r}_1^2-\boldsymbol{r}_2^2\right)\right]exp\left[\frac{ik}{B}\left(\boldsymbol{r}_1\cdot\boldsymbol{\rho}_1-\boldsymbol{r}_2\cdot\boldsymbol{\rho}_2\right)\right]d^2\boldsymbol{r}_1d^2\boldsymbol{r}_2, \tag{19}$$

where $\boldsymbol{\rho_1}=(\boldsymbol{\rho}_{x1},\boldsymbol{\rho}_{y1})$ and $\boldsymbol{\rho_2}=(\boldsymbol{\rho}_{x2},\boldsymbol{\rho}_{y2})$ are two arbitrary transverse position vectors in the observation plane, and A, B, C, D are the transfer matrix elements of an optical system. On substituting **Equation 14** into **Equation 19**, we obtain the analytical formulae for the CSD of a THGCSM beam in the output plane as follows:

$$W(\rho_1,\rho_2;z)=\frac{\pi^2}{\lambda^2B^2\alpha_1\alpha_2}\exp\left[-\frac{\beta_x^2+\beta_y^2}{4\alpha_2}\right]\exp\left[-\frac{ikD}{2B}\left(\rho_1^2-\rho_2^2\right)\right]\exp\left[-\frac{k^2}{4\alpha_1B^2}\left(\rho_1-\rho_2\right)^2\right]\times\sum_{k_1=0}^{m}\sum_{k_2=0}^{n}\sum_{p_1=0}^{k_1}\sum_{p_2=0}^{k_2}\frac{m!\sqrt{\pi}}{\Gamma(m+1/2)}\frac{n!\sqrt{\pi}}{\Gamma(n+1/2)}\frac{(2k_1)}{(2k_1-2p_1)!p_1!}\frac{(2k_2)}{(2k_2-2p_2)!p_2!}\frac{(-1)^{k_1+k_2}}{k_1!k_2!}\times\binom{n-\frac{1}{2}}{n-k_2}\binom{m-\frac{1}{2}}{m-k_1}\left(\frac{1}{2\delta_0^2}\right)^{k_1+k_2}\left(\frac{\beta_x}{2\alpha_2}\right)^{2k_1}\left(\frac{\beta_y}{2\alpha_2}\right)^{2k_2}\left(\frac{\alpha_2}{\beta_x^2}\right)^{p_1}\left(\frac{\alpha_2}{\beta_y^2}\right)^{p_2}, \tag{20}$$

with

$$\alpha_1=\frac{1}{2\sigma_0^2};\ \alpha_2=\frac{1}{8\sigma_0^2}+\frac{1}{2\delta_0^2}+\frac{k^2\mu_0^2}{4\alpha_1}+\frac{k^2A^2}{4\alpha_1B^2}, \tag{21}$$

$$\beta_x=\frac{ik\left(\rho_{x1}+\rho_{x2}\right)}{2B}+\frac{k^2\mu_0\left(\rho_{y1}-\rho_{y2}\right)}{2\alpha_1B}+\frac{k^2A\left(\rho_{x1}-\rho_{x2}\right)}{2\alpha_1B^2}, \tag{22}$$

$$\beta_y=\frac{ik\left(\rho_{y1}+\rho_{y2}\right)}{2B}-\frac{k^2\mu_0\left(\rho_{x1}-\rho_{x2}\right)}{2\alpha_1B}+\frac{k^2A\left(\rho_{y1}-\rho_{y2}\right)}{2\alpha_1B^2} \tag{23}$$

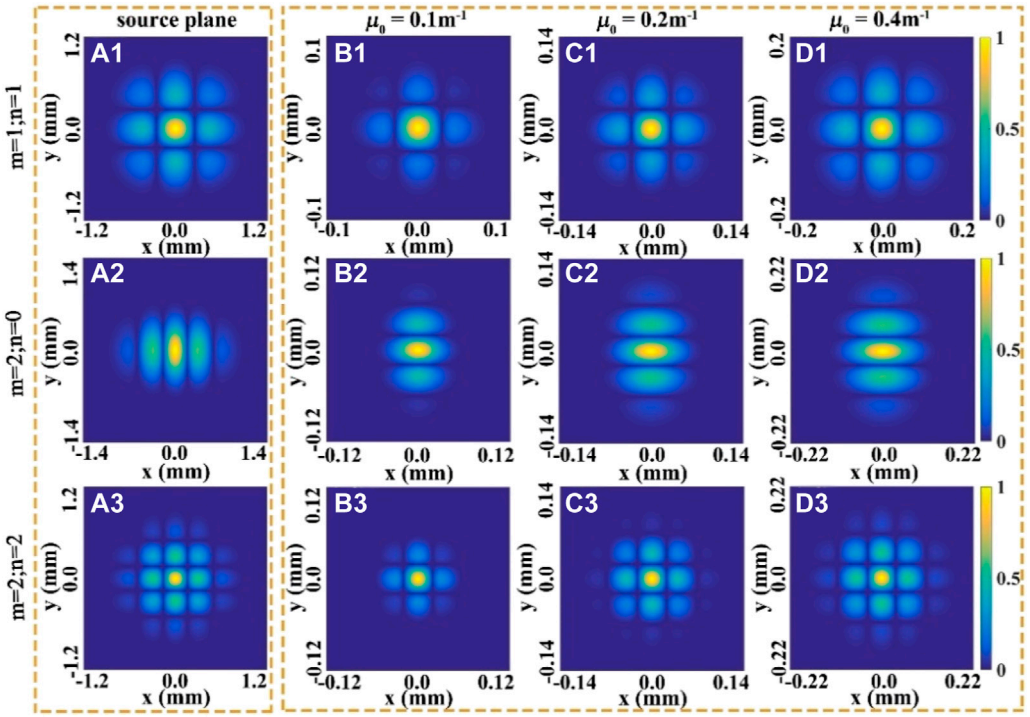

FIGURE 6 | Modulus of the SDOC ($|\eta(\boldsymbol{\rho},-\boldsymbol{\rho})|$) of the THGCSM beam for different values of the twist factor μ_0 in the source and focal plane, respectively.

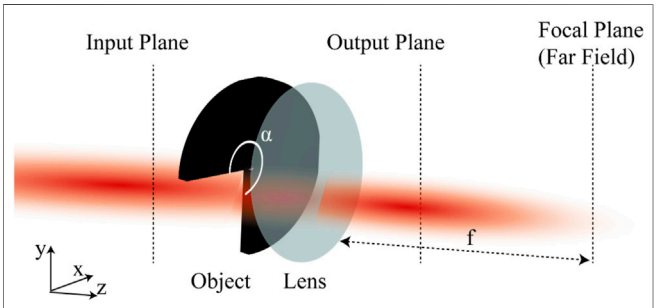

FIGURE 7 | Illustration of a THGCSM beam self-healing process.

The spectral density of the THGCSM beam at point $\boldsymbol{\rho}$ in the receiver plane is defined as

$$S(\boldsymbol{\rho}, z) = W(\boldsymbol{\rho}, \boldsymbol{\rho}, z). \tag{24}$$

The spectral degree of coherence (SDOC) of the THGCSM beam at a pair of transverse points with position vectors $\boldsymbol{\rho_1}$ and $\boldsymbol{\rho_2}$ in the output plane can be expressed by the formula

$$\eta(\boldsymbol{\rho}_1, \boldsymbol{\rho}_2; z) = \frac{W(\boldsymbol{\rho}_1, \boldsymbol{\rho}_2; z)}{\sqrt{W(\boldsymbol{\rho}_1, \boldsymbol{\rho}_1; z) W(\boldsymbol{\rho}_2, \boldsymbol{\rho}_2; z)}} \tag{25}$$

Based on the obtained formulae above, we can study the propagation properties of a THGCSM beam in a convenient way.

NUMERICAL SIMULATION OF A THGCSM BEAM

Paraxial Propagation of the THGCSM Beam Through an ABCD Optical System.

In this section, we study the paraxial propagation of the THGCSM beam through an ABCD optical system by applying the formulae derived in **section 2**. In the following examples, we consider the beam propagating in free space after passing through a lens with focal length $f = 400$mm, which is located at $z = 0$. The parameters of the beam and the transfer matrix are defined as $\lambda = 632.8\ nm$, $\sigma_0 = 1$ mm, $\delta_0 = 0.5$ mm, $A = 1 - z/f$, $B = z$, $C = -1/f$, and $D = 1$. According to **Equation 24**, we calculate the normalized spectral density of a focused THGCSM beam at several propagation distances with different values of the twist factor μ_0, as shown in **Figures 1**, **2**. One can find that when $\mu_0 = 0\ \text{m}^{-1}$ (see the first row), the THGCSM beam reduces to a HGCSM beam, and with the increase of the propagation distance, the intensity distributions of the HGCSM beam gradually change from one beam spot into two spots or four beam spots as expected [22]. From the second and third rows of **Figures 1**, **2,** it is interesting to find that a twist phase does not seem to cause the beam to rotate during the transmission, no matter what the value of the parameters m n is. This result is quite different from that obtained in former works [37, 38], where it was shown that the twist phase would induce the beam to rotate on propagation. This phenomenon will be explained in **Figure 8**, by investigating the self-reconstruction characteristics of the beam spectral density. In addition, the

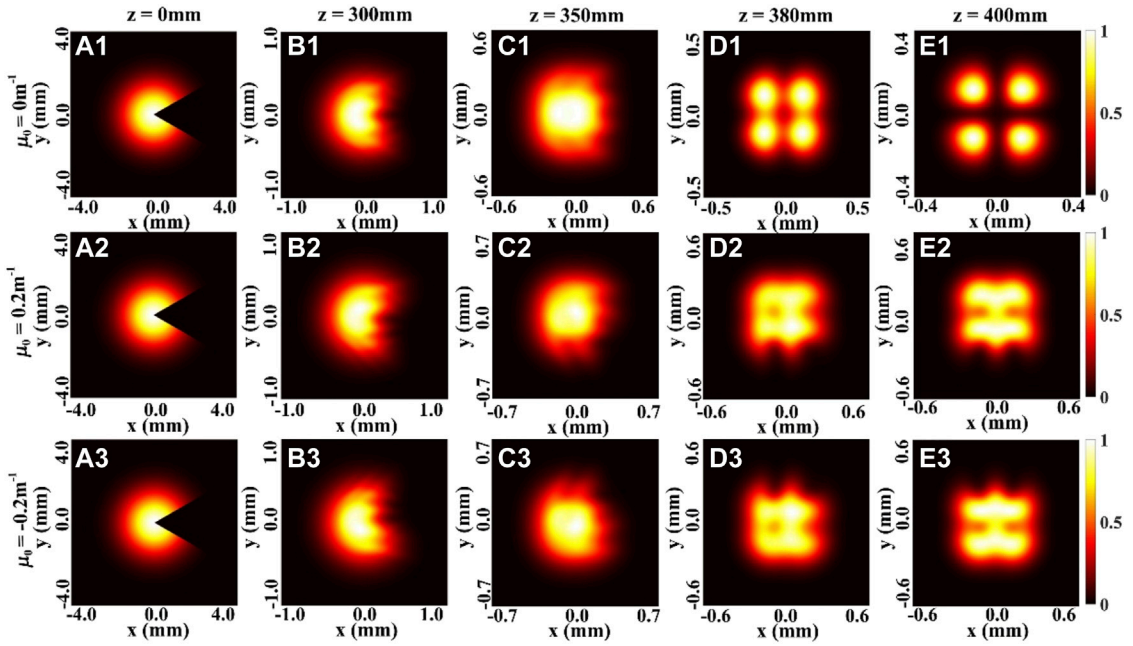

FIGURE 8 | Density plot of the normalized spectral density of a focused THGCSM beam with $m = 1$, $n = 1$ obstructed by a SSOO with center angle $\alpha = \pi/3$ for different values of the twist factor μ_0 at several propagation distances.

twist phase has the effect of hindering the beam spot to split on propagation, and the larger the value of the twist factor is, the beam spot will split more difficult. This means that the twist phase plays a role preventing deterioration of the intensity distribution. Thus, the twist phase can be used to control the intensity distribution of a THGCSM beam on propagation in free space.

Then, the evolution properties the SDOC of a focused THGCSM beam on propagation also have been investigated. **Figures 3**, **4** show the modulus of the SDOC between two points $\boldsymbol{\rho}$ and $-\boldsymbol{\rho}$ (i.e., $|\eta(\boldsymbol{\rho},-\boldsymbol{\rho})|$), at several propagation distances with different values of the twist factor μ_0. The first row of the **Figures 3**, **4** show the variation of the SDOC of a focused HGCSM beam versus the propagation distances z. It is found that the distribution of the SDOC of the HGCSM beam exhibits an array distribution in the source plane (i.e., $z = 0$ mm), and the number of the beamlets increase as the values of the beam order m or n increase.

When the propagation distance z increases, the profile of the SDOC firstly remains invariant, and then becomes one beam spot in the focal plane. This means that the information regarding the SDOC is increasingly lacking with increasing propagation distance. The second and the third rows of the **Figures 3**, **4** show the influence of the twist phase on the evolution properties of the SDOC. We find that the twist phase induces a rotation of the SDOC on propagation, such that when $\mu_0 > 0$, the distribution of the SDOC rotates anti-clockwise, and when $\mu_0 < 0$, the distribution of the SDOC rotates clockwise. The SDOC rotates faster with increasing twist factor μ_0, and the rotation angle varies between $-\pi/2$ or $\pi/2$ in the focal plane. These phenomena can be explained by the fact that the twist phase imposes angular momentum on the beam. Further, one can still determine the structure of the SDOC even in the focal plane. Thus, the twist phase can be used to maintain the beam's information of the correlation function.

In order to investigate the influence of the spatial coherence width and the twist phase on the beam propagation properties, the density plots of the normalized spectral density and the modulus of the SDOC have been studied, as shown in **Figures 5**, **6**. In **Figure 5**, we calculated the density plots of the normalized spectral density and the modulus of the SDOC ($|\eta(\boldsymbol{\rho},-\boldsymbol{\rho})|$) of a focused HGCSM beam (i.e., THGCSM beam with $\mu_0 = 0$) for different values of the spatial coherence width δ_0 in the focal plane. One can find that with the increase of the spatial coherence width, the beam profile of the HGCSM beam will evolve from the original array beam shape to a Gaussian beam profile (i.e., the self-splitting properties of the HGCSM beam on propagation gradually disappear) as expected in [22].

Moreover, regardless of the value of the spatial coherence width, the distribution of the SDOC is always maintained as a beam spot. Therefore, the ability to obtain information about the correlation function of the beam in the far field (or focal plane) cannot be improved by changing the coherence length or the order m n of the beam.

Further, we calculated the modulus of the SDOC ($|\mu(\boldsymbol{\rho},-\boldsymbol{\rho})|$) of the THGCSM beam in the source and focal plane, respectively. It is interesting to find that with the increase of the twist factor, the strength of the sidelobes of the SDOC are

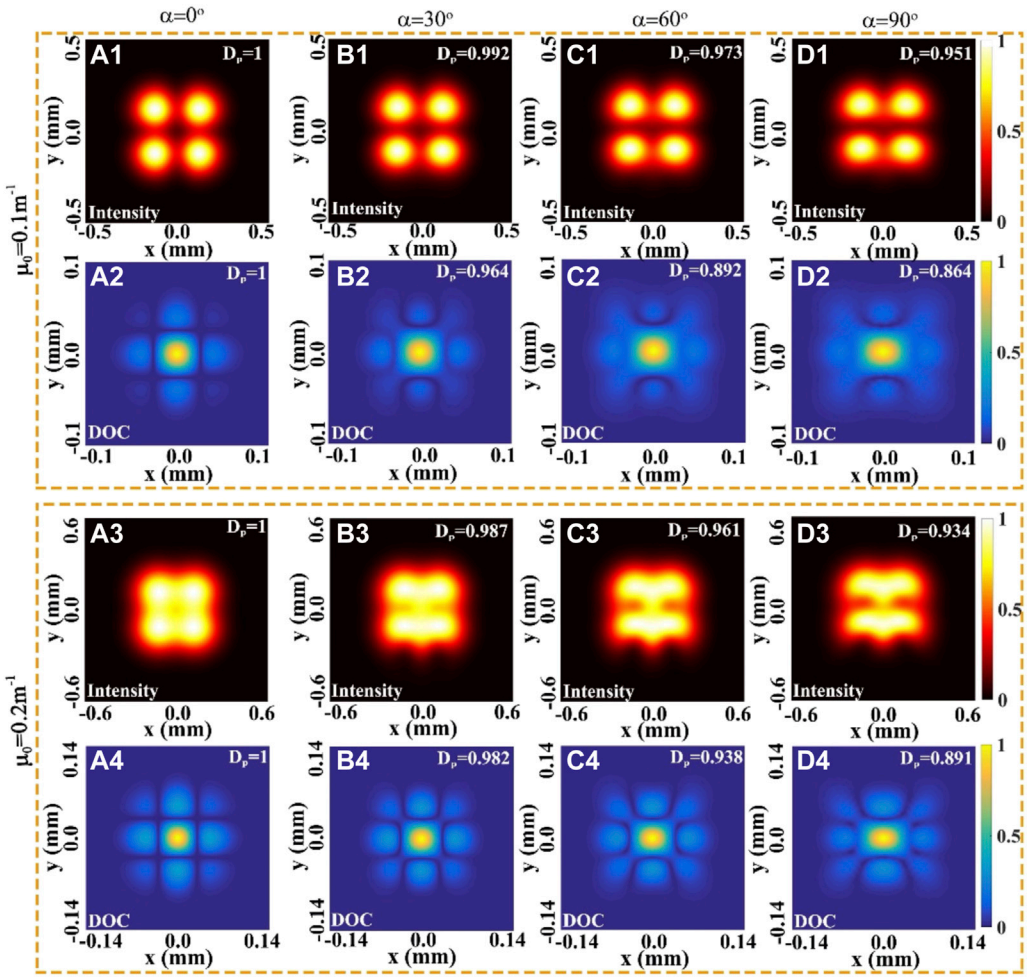

FIGURE 9 | Density plot of the normalized spectral density and the modulus of the SDOC ($|\eta(\boldsymbol{\rho},-\boldsymbol{\rho})|$) of a focused THGCSM beam with $m = 1$, $n = 1$ obstructed by a SSOO for different values of twist factor μ_0 and center angle α in the focal plane.

enhanced. This exciting new finding may help us to find a new way to improve the reliability of the correlation function.

Self-Reconstruction Characteristics of the THGCSM Beam

In this section, we focus on the Self-reconstruction behavior of the THGCSM beam when the THGCSM beam is partially blocked by a sector-shaped opaque obstacle (SSOO) in the source plane. **Figure 7** shows the illustration of a THGCSM beam self-healing process. A beam in the input plane ($z = 0$) is disturbed by a partially opaque obstacle in the input plane and is propagating through an ABCD optical system consisting of a lens and the free space behind the lens.

Figure 8 shows the changes of the density plot of the normalized spectral density of a focused THGCSM beam obstructed by a SSOO for different values of the twist factor at several propagation distances. From the first row of the **Figure 8**, one can see that with the increase of the propagation distance z, due to the effect of the correlation function, the beam splits into four beamlets as expected in [22]. The second and third row of the **Figure 8** show the effect of the twist phase on the normalized spectral density. By comparing the condition $\mu_0 = 0.2\ \mathrm{m}^{-1}$ and the condition $\mu_0 = -0.2\ \mathrm{m}^{-1}$, we can find that the twist phase would induce the rotation of the beam on propagation: the distribution of the spectral density rotates clockwise when $\mu_0 > 0$, the distribution of the spectral density rotates anti-clockwise when $\mu_0 < 0$. This phenomenon is consistent with former results [37, 38]. Therefore, the twist phase actually still causes the beam to rotate during propagation, but it is not noticeable when the beam is intact (**Figures 1**, **2**).

Moreover, **Figure 9** shows the Self-reconstruction characteristics of the normalized spectral density and the modulus of the SDOC ($|\eta\boldsymbol{\rho},-\boldsymbol{\rho})|$) when the beam is obstructed by a SSOO for different values of the center angle α in the focal plane. To assess the influences of the twist parameter on the self-

reconstruction capability quantitatively, a parameter named the degree of self-reconstruction D_P (i.e., $D_p = \frac{\left[\iint \langle I_{wt}(\boldsymbol{\rho})\rangle\langle I_{ob}(\boldsymbol{\rho})\rangle d^2\boldsymbol{\rho}\right]^2}{\iint \langle I_{wt}(\boldsymbol{\rho})^2\rangle d^2\boldsymbol{\rho} \iint \langle I_{ob}(\boldsymbol{\rho})^2\rangle d^2\boldsymbol{\rho}}$, with I_{wt} and I_{ob} stand for the beam intensities without and with obstruction, respectively) is used to characterize it [41]. It is interesting to find that even if the beam has been obstructed by a SSOO, one still can determine the information of the correlation function of an obstructed THGCSM from its SDOC distribution in the focal plane. In addition, with the increase of the center angle, the self-reconstruction capability also decreased (see the evolution of the quantity D_P in the left upper corner of the figure). Our results can find application in information transmission and recovery.

CONCLUSION

In summary, we have introduced a new class of partially coherent twisted beam, named twisted Hermite-Gaussian correlated Schell-model (THGCSM) beam, and investigated its propagation properties through an ABCD optical system. The problem of when a twist phase can be imposed on Schell-model source fields with rectangular symmetries was solved. Based on the derived assessment condition, the condition that the THGCSM beam will be a bona fide one, also has been explored. The analytical expression for the CSD function of the THGCSM propagation through an ABCD optical system has been derived with the help of the generalized Collins integral formula. Based on the derived formula we have examined the evolution properties of the THGCSM beam. Our simulation results indicate that the evolution properties of the beam are closely related to the twist phase, e.g., with an increasing twist phase, the self-splitting properties of the beam gradually weaken on propagation. Further, the evolution of the SDOC also has been studied. Apart from inducing the rotation of the SDOC on propagation, the twist phase can greatly enhance the ability of the SDOC to maintain its profile on propagation, even in the focal plane. This provides a way to improve the reliability of the correlation function. Moreover, the self-reconstruction characteristics of the THGCSM beam have been explored in detail, and one can find that even if the beam has been obstructed by an opaque obstacle, one still can determine the information relating to the correlation function of an obstructed THGCSM from its SDOC distribution in the focal plane. Our results are anticipated to find applications in optical communications and information recovery.

DATA AVAILABILITY STATEMENT

The original contributions presented in the study are included in the article/Supplementary Material, further inquiries can be directed to the corresponding authors.

AUTHOR CONTRIBUTIONS

LeL and XP proposed the idea. LeL wrote the original manuscript. HW, LiL, YD, and FW gave suggestions in numerical simulation. XP, YC, and BH supervised the project. All authors contributed to the revision of the manuscript and approved the final version.

FUNDING

This work was supported by the National Natural Science Foundation of China (Nos 12192254, 11774251, 11874046, 11904247, 11974218, 12104263, 12174279); National Key Research and Development Program of China (2019YFA0705000); Natural Science Foundation of Shandong Province (ZR2021QA093); Local Science and Technology Development Project of the Central Government (Grant No. YDZX20203700001766); Innovation Group of Jinan (2018GXRC010).

REFERENCES

1. Kato Y, Mima K, Miyanaga N, Arinaga S, Kitagawa Y, Nakatsuka M, et al. Random Phasing of High-Power Lasers for Uniform Target Acceleration and Plasma-Instability Suppression. *Phys Rev Lett* (1984) 53:1057–60. doi:10.1103/PhysRevLett.53.1057
2. Ferri F, Magatti D, Gatti A, Bache M, Brambilla E, Lugiato LA. High-resolution Ghost Image and Ghost Diffraction Experiments with thermal Light. *Phys Rev Lett* (2005) 94:183602. doi:10.1103/PhysRevLett.94.183602
3. Oh J-E, Cho Y-W, Scarcelli G, Kim Y-H. Sub-Rayleigh Imaging via Speckle Illumination. *Opt Lett* (2013) 38:682–4. doi:10.1364/OL.38.000682
4. Auñón JM, Nieto-Vesperinas M. Partially Coherent Fluctuating Sources that Produce the Same Optical Force as a Laser Beam. *Opt Lett* (2013) 38:2869–72. doi:10.1364/OL.38.002869
5. Zhao C, Cai Y. Trapping Two Types of Particles Using a Focused Partially Coherent Elegant Laguerre-Gaussian Beam. *Opt Lett* (2011) 36:2251–3. doi:10.1364/OL.36.002251
6. Ricklin JC, Davidson FM. Atmospheric Optical Communication with a Gaussian Schell Beam. *J Opt Soc Am A* (2003) 20:856–66. doi:10.1364/josaa.20.000856
7. Beams R, Cançado LG, Oh S-H, Jorio A, Novotny L. Spatial Coherence in Near-Field Raman Scattering. *Phys Rev Lett* (2014) 113:186101. doi:10.1103/PhysRevLett.113.186101
8. van Dijk T, Fischer DG, Visser TD, Wolf E. Effects of Spatial Coherence on the Angular Distribution of Radiant Intensity Generated by Scattering on a Sphere. *Phys Rev Lett* (2010) 104:173902. doi:10.1103/PhysRevLett.104.173902
9. Gori F, Santarsiero M. Devising Genuine Spatial Correlation Functions. *Opt Lett* (2007) 32:3531–3. doi:10.1364/ol.32.003531
10. Gori F, Ramírez-Sánchez V, Santarsiero M, Shirai T. On Genuine Cross-Spectral Density Matrices. *J Opt A: Pure Appl Opt* (2009) 11:085706. doi:10.1088/1464-4258/11/8/085706
11. Cai Y, Chen Y, Yu J, Liu X, Liu L. Generation of Partially Coherent Beams. *Prog Opt* (2017) 62:157–223. doi:10.1016/bs.po.2016.11.001
12. Cai Y, Chen Y, Wang F. Generation and Propagation of Partially Coherent Beams with Nonconventional Correlation Functions: A Review [invited]. *J Opt Soc Am A* (2014) 31:2083–96. doi:10.1364/JOSAA.31.002083

13. Lajunen H, Saastamoinen T. Propagation Characteristics of Partially Coherent Beams with Spatially Varying Correlations. *Opt Lett* (2011) 36:4104–6. doi:10.1364/OL.36.004104
14. Wang F, Liu X, Yuan Y, Cai Y. Experimental Generation of Partially Coherent Beams with Different Complex Degrees of Coherence. *Opt Lett* (2013) 38:1814–6. doi:10.1364/OL.38.001814
15. Mei Z, Korotkova O. Random Sources Generating Ring-Shaped Beams. *Opt Lett* (2013) 38:91–3. doi:10.1364/OL.38.000091
16. Mei Z, Korotkova O. Cosine-Gaussian Schell-Model Sources. *Opt Lett* (2013) 38:2578–80. doi:10.1364/OL.38.002578
17. Liang C, Wang F, Liu X, Cai Y, Korotkova O. Experimental Generation of Cosine-Gaussian-Correlated Schell-Model Beams with Rectangular Symmetry. *Opt Lett* (2014) 39:769–72. doi:10.1364/OL.39.000769
18. Chen Y, Cai Y. Generation of a Controllable Optical Cage by Focusing a Laguerre-Gaussian Correlated Schell-Model Beam. *Opt Lett* (2014) 39:2549–52. doi:10.1364/OL.39.002549
19. Korotkova O. Random Sources for Rectangular Far fields. *Opt Lett* (2014) 39:64–7. doi:10.1364/OL.39.000064
20. Chen Y, Wang F, Liu L, Zhao C, Cai Y, Korotkova O. Generation and Propagation of a Partially Coherent Vector Beam with Special Correlation Functions. *Phys Rev A* (2014) 89:13801. doi:10.1103/PhysRevA.89.013801
21. Ma L, Ponomarenko SA. Free-space Propagation of Optical Coherence Lattices and Periodicity Reciprocity. *Opt Express* (2015) 23:1848–56. doi:10.1364/OE.23.001848
22. Chen Y, Gu J, Wang F, Cai Y. Self-splitting Properties of a Hermite-Gaussian Correlated Schell-Model Beam. *Phys Rev A* (2015) 91:13823. doi:10.1103/PhysRevA.91.013823
23. Zhu S, Chen Y, Wang J, Wang H, Li Z, Cai Y. Generation and Propagation of a Vector Cosine-Gaussian Correlated Beam with Radial Polarization. *Opt Express* (2015) 23:33099–155. doi:10.1364/OE.23.033099
24. Chen Y, Ponomarenko SA, Cai Y. Experimental Generation of Optical Coherence Lattices. *Appl Phys Lett* (2016) 109:061107. doi:10.1063/1.4960966
25. Liu X, Yu J, Cai Y, Ponomarenko SA. Propagation of Optical Coherence Lattices in the Turbulent Atmosphere. *Opt Lett* (2016) 41:4182–5. doi:10.1364/OL.41.004182
26. Liang C, Mi C, Wang F, Zhao C, Cai Y, Ponomarenko SA. Vector Optical Coherence Lattices Generating Controllable Far-Field Beam Profiles. *Opt Express* (2017) 25:9872–85. doi:10.1364/OE.25.009872
27. Xu Z, Liu X, Chen Y, Wang F, Liu L, Monfared YE, et al. Self-healing Properties of Hermite-Gaussian Correlated Schell-Model Beams. *Opt Express* (2020) 28:2828–37. doi:10.1364/OE.383805
28. Gu Y, Gbur G. Scintillation of Nonuniformly Correlated Beams in Atmospheric Turbulence. *Opt Lett* (2013) 38:1395–7. doi:10.1364/OL.38.001395
29. Liang C, Wu G, Wang F, Li W, Cai Y, Ponomarenko SA. Overcoming the Classical Rayleigh Diffraction Limit by Controlling Two-point Correlations of Partially Coherent Light Sources. *Opt Express* (2017) 25:28352–62. doi:10.1364/OE.25.028352
30. Peng D, Huang Z, Liu Y, Chen Y, Wang F, Ponomarenko SA, et al. Optical Coherence Encryption with Structured Random Light. *PhotoniX* (2021) 2:6–15. doi:10.1186/s43074-021-00027-z
31. Shen Y, Sun H, Peng D, Chen Y, Cai Q, Wu D, et al. Optical Image Reconstruction in 4f Imaging System: Role of Spatial Coherence Structure Engineering. *Appl Phys Lett* (2021) 118:181102. doi:10.1063/5.0046288
32. Liu Y, Chen Y, Wang F, Cai Y, Liang C, et al. Robust Far-Field Imaging by Spatial Coherence Engineering. *Opto-Electron Adv* (2021) 4:210027. doi:10.29026/oea.2021.210027
33. Chen Y, Wang F, Cai Y. Partially Coherent Light Beam Shaping via Complex Spatial Coherence Structure Engineering. *Adv Phys X* (2022) 7:2009742. doi:10.1080/23746149.2021.2009742
34. Serna J, Movilla JM. Orbital Angular Momentum of Partially Coherent Beams. *Opt Lett* (2001) 26:405–7. doi:10.1364/OL.26.000405
35. Simon R, Mukunda N. Twisted Gaussian Schell-Model Beams. *J Opt Soc Am A* (1993) 10:95. doi:10.1364/JOSAA.10.000095
36. Friberg AT, Tervonen E, Turunen J. Interpretation and Experimental Demonstration of Twisted Gaussian Schell-Model Beams. *J Opt Soc Am A* (1994) 11:1818–26. doi:10.1364/JOSAA.11.001818
37. Peng X, Liu L, Yu J, Liu X, Cai Y, Baykal Y, et al. Propagation of a Radially Polarized Twisted Gaussian Schell-Model Beam in Turbulent Atmosphere. *J Opt* (2016) 18:125601. doi:10.1088/2040-8978/18/12/125601
38. Wu G. Propagation Properties of a Radially Polarized Partially Coherent Twisted Beam in Free Space. *J Opt Soc Am A* (2016) 33:345–50. doi:10.1364/JOSAA.33.000345
39. Tong Z, Korotkova O. Beyond the Classical Rayleigh Limit with Twisted Light. *Opt Lett* (2012) 37:2595–7. doi:10.1364/OL.37.002595
40. Peng X, Liu L, Wang F, Popov S, Cai Y. Twisted Laguerre-Gaussian Schell-Model Beam and its Orbital Angular Moment. *Opt Express* (2018) 26:33956–69. doi:10.1364/OE.26.033956
41. Peng X, Wang H, Liu L, Wang F, Popov S, Cai Y. Self-reconstruction of Twisted Laguerre-Gaussian Schell-Model Beams Partially Blocked by an Opaque Obstacle. *Opt Express* (2020) 28:31510–23. doi:10.1364/OE.408357
42. Wang H, Peng X, Liu L, Wang F, Cai Y, Ponomarenko SA. Generating Bona Fide Twisted Gaussian Schell-Model Beams. *Opt Lett* (2019) 44:3709–12. doi:10.1364/OL.44.003709
43. Wang H, Peng X, Zhang H, Liu L, Chen Y, Wang F, et al. Experimental Synthesis of Partially Coherent Beam with Controllable Twist Phase and Measuring its Orbital Angular Momentum. *Nanophotonics* (2021). doi:10.1515/nanoph-2021-0432
44. Borghi R. Twisting Partially Coherent Light. *Opt Lett* (2018) 43:1627–30. doi:10.1364/OL.43.001627
45. Borghi R, Gori F, Guattari G, Santarsiero M. Twisted Schell-Model Beams with Axial Symmetry. *Opt Lett* (2015) 40:4504. doi:10.1364/OL.40.004504
46. Mei Z, Korotkova O. Random Sources for Rotating Spectral Densities. *Opt Lett* (2017) 42:255–8. doi:10.1364/OL.42.000255
47. Gori F, Santarsiero M. Devising Genuine Twisted Cross-Spectral Densities. *Opt Lett* (2018) 43:595–8. doi:10.1364/OL.43.000595
48. Wolf E. *Introduction to the Theory of Coherence and Polarization of Light [M]*. Cambridge: Cambridge University Press (2007).

Conflict of Interest: The authors declare that the research was conducted in the absence of any commercial or financial relationships that could be construed as a potential conflict of interest.